Mechanics of Composite Materials, Vol. 41, No. 2, 2005

DESIGN OF STEEL-COMPOSITE MULTIRIM CYLINDRICAL FLYWHEELS MANUFACTURED BY WINDING WITH HIGH TENSIONING AND *IN SITU* CURING. 1. BASIC RELATIONS

G. Portnov,* A.-N. Uthe, I. Cruz,*****
R. P. Fiffe,* and F. Arias*****

Keywords*: hybrid flywheel, winding, tensioning, in situ curing, stress state, energy storage capacity*

The possibility of using force winding coupled with in situ curing to increase the energy storage capacity of hybrid steel-composite cylindrical flywheels is estimated and analyzed. Relations describing the rotational, thermal, and winding stresses are considered and discussed. These relations are used for a numerical analysis of the stress state and energy capacity of hybrid flywheels in the second part of the paper.

1. Introduction

In this paper, the efficiency of a possible composite flywheel design is analyzed. In the late 1970s and early 1980s, much research on composite flywheels was carried out in response to the energy storage needs in space and automotive applications, resulting in an abundance of competing designs on drawing boards [1-3]. The research into flywheels has recently resurged to meet the needs of power companies, low- or zero-emission automobiles, and uninterrupted power supplies [4]. These investigations are worth mentioning because flywheels enable the reduction of greenhouse gases and poisonous chemical emissions [5, 6]. The potential advantages and fields of applications of flywheel energy storage systems are described, for example, in [7-10].

Among the composite material designs promulgated were flat laminated disks, tapered-thickness disks, flat laminated disks with filament-wound overwraps, spoked or disklike metallic hubs with single or multiple filament-wound rings, multiple concentric rings separated by a compliant material, unidirectional rods spun about a mass centre, elastomer-matrix filament-wound rings, and polar-woven resin transfer molded rings, to name a few. Without doubt, the immense design flexibility made possible by the modern composite-material manufacture technology has given rise to many potentially viable alternatives.

The experience accumulated shows that the most effective state-of-the-art flywheels have a circumferentially wound ring (or rings) as the main energy-storage element [11]. A circumferentially wound ring, which exhibits the highest strength in

---

*Institute of Polymer Mechanics, University of Latvia, Riga, LV-1006, Latvia. **Technical University of Dresden, Dresden, Germany. ***Research Center for Energy, Enviroment, and Technology, Department of Renewable Energies (CIEMAT-DER), Madrid, Spain. Russian translation published in Mekhanika Kompozitnykh Materialov, Vol. 41, No. 2, pp. 203-224, March-April, 2005. Original article submitted December, 13, 2004.

0191-5665/05/4102-0139

the θ direction, due to its low transverse tensile strength F_r^+, is applicable only to a thin rim. Overcoming the problem of radial stresses is one of the most important issues in high-speed composite flywheels. There are two approaches to coping with this problem. One is to reduce the radial stresses σ_r, and another is to raise the radial strength F_r^+.

A successful and common way to reduce the radial stresses is the employment of the multiring concept. Even though the maximum radial stresses in a thick single ring and in two similar rings with the total thickness equal to the thickness of the single ring exceed the ultimate radial strength, two rings connected with press fit or consisting of different materials can have compressive radial stresses. In other words, the ring having a low specific modulus produces a compressive force on the outer, stiffer ring. Depending on the materials chosen, the inner radius of each ring enables us to change the stress distribution dramatically. Since this approach is used in the given paper, the investigations connected with the multiring or the hybrid flywheel concept will be considered in more detail.

2. Literature Review

Among the multiring design approaches are the following ones: (a) using one or several less stiff rings inside the outer ring to provide an outward pressure as the rotational speed increases [12-14]; (b) using press-fit multiple rings to superimpose a compressive radial stress field onto the tensile field caused by rotation [13, 15, 16]; (c) using solid, compliant, radial elastomeric interlayers to relieve the radial stress transfer from one ring to the adjacent one [17-19]. Special cases of all these designs can be analyzed using elasticity solutions or the FEM, providing that the basic material and geometric stipulations are met and the compatibility is ensured at all interfaces. A review of works devoted to different types of rotating disks is presented in [13]. In this paper, a broad classification of previous investigations in the field of composite disks is cited. The calculation of a multiring flywheel, by itself, is not a complicated problem. The complexity of the problem, as shown in this work, lies in the fact that a very large number of conditions and factors must be taken into account. In particular, in the case of rotating multiring disks, the relative thickness of the rings, their materials, and the press fits generating the initial stresses must be considered and simultaneously optimized to obtain a most effective, with respect to the stored energy, and a most reliable design. At the same time, practically each of the investigations mentioned in the review is necessarily focused on some specific conditions, particular materials, and related conditions.

Summing up the results of investigations of hybrid-type flywheels, it should be pointed out, that a consequent policy of their optimal design is practically absent. Usually the selection of a best design is realized by simply enumerating its possibilities. So even a well-reasoned selection of a first approximation of an efficient material sequence and the thickness of layers (rings and cylinders) is of considerable interest for designers.

Another problem is the account of residual (initial) stresses. The point is that, during the manufacture of thick wound hoop rings, significant residual stresses can form in them as a result of complex interactions of winding tensioning, matrix viscosity and stiffness, cure shrinkage, and thermal expansions. These residual stresses in highly anisotropic rings can be large enough to cause matrix cracking in some instances, especially in the case of hybrid flywheels. At the same time, only in [20] the initial thermal stresses due to the cooling after curing of composite rings were taken into account.

One of the methods for superimposing a compressive radial stress field onto the tensile field caused by rotation is the use of press-fit multiple rings, as was mentioned above. But, for the same purpose, the force winding can also be used. The calculation of either type of initial stresses (thermal and from the force winding) is needed to consider the winding technology. At the moment, the most advanced winding technology is employed, namely the winding with *in situ* gelation (or curing).

3. Problem Statement

The investigation presented in this paper originated from the necessity to design a kinetic-energy storage system (KESS) for an isolated wind power generator developed in CIEMAT [21]. The flywheel has to ensure the accumulation of 1.25-kWh energy with a peak power of 50 kW and an operating speed between 10,000 and 30,000 rpm. The mass of the fly-

wheel is not of decisive importance, since the KESS is stationary, but a possible decrease in mass is desirable. More important questions are the cost of the flywheel and the simplicity of its manufacture.

The high speed of rotation presents problems for the use of a pure steel flywheel. Such a flywheel must be too long in the axial direction to accumulate the necessary amount of energy. In order to lower the cost of the flywheel, it is desirable to make it in one sitting, without (or almost without) subsequent assembling.

At the first sight, from the engineering point of view, such requirements can be satisfied using a compound flywheel: an inner steel cylinder wrapped with a glass-fiber-reinforced plastic (GRP) and a carbon-reinforced plastic (CRP). In such a way, the inner steel cylinder, with its ends adapted for connection to a shaft, is utilized simultaneously as a mandrel during the winding of outer cylinders. The aim of this research is to estimate the efficiency of this design.

The main problems in such a construction, as shown by the existing experience in flywheel design, are associated with the low resistance of composites to the radial tensile stresses. The main part of these stresses are generated during rotation, owing to the different stiffnesses of the coupled steel and composite cylinders. Another their part is created at rest, after cooling the manufactured cylinders, owing to the initial thermal stresses in each of the thick composite cylinders and to the coupling of cylinders with different thermal-expansion coefficients.

The components of a compound composite flywheel are usually made separately and then are connected using previously calculated press fits to suppress the dangerous radial tensile stresses. In our case, the use of winding with high tensioning (force winding) created by a prestressed construction instead of press fits is considered.

The main subjects of this investigation, which distinguishes it from the most of previous works in the field, are as follows:

— transition from a disk-type to a cylindrical compound flywheel design (from a plane stress state to a plain strain state);

— taking into account the technological prehistory of the flywheel (the thermal and winding stresses created during the manufacture of a flywheel).

4. Thermal and Rotational Stresses in an Anisotropic Cylinder

4.1 Basic equations. The basic calculations in optimizing a hybrid flywheel are connected with determination of stresses and radial displacements in an anisotropic cylinder. The cylinder is free at its ends and can expand in the axial direction. Furthermore, the materials are cylindrically orthotropic and are loaded with axisymmetric stresses caused by rotation and temperature changes from the cure temperature to room temperature. First, we utilize the radial equilibrium equation for a cylinder in an axisymmetric plane state under centrifugal forces. The same equation is valid for plane stress and strain states, namely

$$\frac{d}{dr}\sigma_r + \frac{\sigma_r - \sigma_\theta}{r} + \rho r\omega^2 = 0, \tag{1}$$

where σ_r and σ_θ are the radial and circumferential stresses, ρ is the mass density, r is the radius, and ω is the angular speed. The strains and stresses are related by the equation of state

$$\varepsilon = C\sigma + \alpha\Delta T, \tag{2}$$

$$\varepsilon = \begin{pmatrix} \varepsilon_\theta \\ \varepsilon_r \\ \varepsilon_z \end{pmatrix}, \quad \sigma = \begin{pmatrix} \sigma_\theta \\ \sigma_r \\ \sigma_z \end{pmatrix}, \quad \alpha = \begin{pmatrix} \alpha_\theta \\ \alpha_r \\ \alpha_z \end{pmatrix},$$

where ε and σ are the strain and stress vectors, and α is the vector of thermal-expansion coefficients; θ stands for the circumferential, r for the radial, and z for the axial directions. The quantity ΔT is to the difference between the room T_r and cure T_c temperatures: $\Delta T = T_\mathrm{r} - T_\mathrm{c}$.

The compliance matrix C is defined by material properties:

$$C = \begin{pmatrix} \frac{1}{E_\theta} & \frac{-\nu_{\theta r}}{E_r} & \frac{-\nu_{\theta z}}{E_z} \\ \frac{-\nu_{r\theta}}{E_\theta} & \frac{1}{E_r} & \frac{-\nu_{rz}}{E_z} \\ \frac{-\nu_{z\theta}}{E_\theta} & \frac{-\nu_{zr}}{E_r} & \frac{1}{E_z} \end{pmatrix}, \quad \nu_{r\theta} = \nu_{\theta r} \frac{E_\theta}{E_r}, \tag{3}$$

where E_i is the elastic modulus in an i-direction, and ν_{ij} is the Poisson ratio, showing the contraction in the i-direction caused by tension in a j-direction.

The strain–displacement relations for the case of axisymmetric plane strain state considered are described by the relations

$$\varepsilon_\theta = \frac{u}{r}, \quad \varepsilon_r = \frac{\partial u}{\partial r}, \quad \varepsilon_z = \frac{\partial w}{\partial z}, \tag{4}$$

where u is the radial displacement, and w is the axial displacement, which is constant along the radius.

The solution method is as follows. The expression for stresses are obtained from Eq. (2),

$$\sigma = Q(\varepsilon - \alpha \Delta T), \tag{5}$$

where Q denotes the stiffness matrix; α is the vector of thermal-expansion coefficients, which will be used in the form $\beta = Q\alpha$. The stiffness matrix Q is inverse to the compliance matrix C:

$$Q = \begin{pmatrix} \frac{1}{E_\theta} & & \text{sym} \\ \frac{-\nu_{r\theta}}{E_\theta} & \frac{1}{E_r} & \\ \frac{-\nu_{z\theta}}{E_\theta} & \frac{-\nu_{zr}}{E_r} & \frac{1}{E_z} \end{pmatrix}. \tag{6}$$

It is assumed that the z-direction axial strain is an unknown constant ε_0 that must be calculated,

$$\varepsilon_z = \varepsilon_0. \tag{7}$$

After substituting Eq. (4) and (5) into Eq. (1), we obtain the governing equation for radial displacements

$$r^2 u'' + r u' - \frac{Q_{11}}{Q_{22}} u = -\frac{Q_{23} - Q_{13}}{Q_{22}} r\varepsilon_0 + \frac{\beta_2 - \beta_1}{Q_{22}} r\Delta T - \frac{\rho r^3 \omega^2}{Q_{22}}. \tag{8}$$

The solution of Eq. (8) consists of the general solution to the corresponding homogeneous equation and three particular solutions to the nonhomogeneous equations:

$$u = C_1 r^k + C_2 r^{-k} + \zeta_1 \varepsilon_0 r + \zeta_2 \Delta T r + \zeta_3 \omega^2 r^3, \tag{9}$$

where C_1, C_2, and ε_0 are unknown constants, which are found from boundary conditions; k and ζ_i depend on material properties:

$$k = \sqrt{\frac{Q_{11}}{Q_{22}}}, \quad \zeta_1 = \frac{Q_{13} - Q_{23}}{Q_{22} - Q_{11}}, \quad \zeta_2 = \frac{\beta_2 - \beta_1}{Q_{22} - Q_{11}}, \quad \zeta_3 = \frac{-\rho}{(9 - k^2) Q_{22}}, \quad \beta = Q\alpha. \tag{10}$$

The current radius r is converted into a dimensionless form by dividing it by the outer radius b of the cylinder:

$$\chi = r/b. \tag{11}$$

After substituting solution (9) in Eqs. (4) and (5), we obtain relations for stresses and displacements, which depend on the dimensionless radius χ and material properties:

$$\begin{aligned}
\sigma_\theta(\chi) &= C_1(Q_{11}+kQ_{12})\chi^{k-1} + C_2(Q_{11}-kQ_{12})\chi^{-k-1} + \varepsilon_0[\zeta_1(Q_{11}+Q_{12})+Q_{13}] + \Delta T[\zeta_2(Q_{11}+Q_{12})-\beta_1] \\
&\quad + \zeta_3\omega^2(Q_{11}+3Q_{12})\chi^2 b^2, \\
\sigma_r(\chi) &= C_1(Q_{12}+kQ_{22})\chi^{k-1} + C_2(Q_{12}-kQ_{22})\chi^{-k-1} + \varepsilon_0[\zeta_1(Q_{12}+Q_{22})+Q_{23}] + \Delta T[\zeta_2(Q_{12}+Q_{22})-\beta_2] \\
&\quad + \zeta_3\omega^2(Q_{12}+3Q_{22})\chi^2 b^2, \\
\sigma_z(\chi) &= C_1(Q_{13}+kQ_{23})\chi^{k-1} + C_2(Q_{13}-kQ_{23})\chi^{-k-1} + \varepsilon_0[\zeta_1(Q_{13}+Q_{23})+Q_{33}] + \Delta T[\zeta_2(Q_{13}+Q_{23})-\beta_3] \\
&\quad + \zeta_3\omega^2(Q_{13}+3Q_{23})\chi^2 b^2, \\
\bar{u}(\chi) &= \frac{u}{b} = C_1\chi^k + C_2\chi^{-k} + \zeta_1\varepsilon_0\chi + \zeta_2\Delta T\chi + \zeta_3\omega^2\chi^3 b^2,
\end{aligned} \tag{12}$$

where σ_θ, σ_r, and σ_z are the stresses in the circumferential, radial, and axial directions, and $\bar{u}$ is the dimensionless radial displacement. If material properties are given, the unknown constants depend upon geometrical dimensions, the temperature change, and the angular speed of the cylinder and are found from boundary conditions. For a freely rotating hybrid cylinder consisting of n elementar cylinders made of different materials, the stresses and displacements in each cylinder are described by Eqs. (12). To determine the $2n+1$ constants ($C_1^{(i)}$, $C_2^{(i)}$, and ε_0), the following conditions are used:

$$\begin{aligned}
&\sigma_r^{(1)}(r^{(1)} = a_1) = \sigma_r^{(1)}(\chi^{(1)} = c_1) = 0, \\
&\sigma_r^{(n)}(r^{(n)} = b_n) = \sigma_r^{(n)}(\chi^{(n)} = 1) = 0, \\
&\sigma_r^{(i)}(r^{(i)} = b_i) = \sigma_r^{(i+1)}(r^{(i+1)} = a_{i+1}) \to \sigma_r^{(i)}(\chi^{(i)} = 1) = \sigma_r^{(i+1)}(\chi^{(i+1)} = c_{i+1}), \quad i = 1\ldots(n-1), \\
&\bar{u}^{(i)}(r^{(i)} = b_i) = \bar{u}^{(i+1)}(r^{(i+1)} = a_{i+1}) \to \bar{u}^{(i)}(\chi^{(i)} = 1) \\
&\quad = \bar{u}^{(i+1)}(\chi^{(i+1)} = c_{i+1}), \quad i = 1\ldots(n-1), \\
&\sum_1^n \int_{a_i}^{b_i} \sigma_z^{(i)} r^{(i)} dr^{(i)} = \sum_1^n \int_{c_i}^{1} b_i^2 \sigma_z^{(i)} \chi^{(i)} d\chi^{(i)} = 0,
\end{aligned} \tag{13}$$

where a_i, b_i, and $r^{(i)}$ are the inner, outer, and current radii of an ith cylinder, $c_i = a_i/b_i$, and $\chi^{(i)} = r^{(i)}/b_i$.

The first two equations in (13) correspond to the conditions of unloaded outer and inner surfaces of the hybrid cylinder, the next two correspond to the conditions of continuity of radial stresses and displacements at the contact surfaces of the cylinders, and the last one corresponds to the condition of zero resultant axial force in the radial cross section of the hybrid cylinder.

Relations (12) and (13) almost coincide with those obtained in [20]. In [20], a disputable assumption of "modified generalized plane strain" is used, according to which the axial strains are expressed as $\varepsilon_z = \varepsilon_0 + \varepsilon_1 r$, where ε_0 and ε_1 are constants, instead of the traditional hypothesis $\varepsilon_0 = \text{const}$.

All calculations were realized using Mathcad 2001. The programs, written in Mathcad, were verified by comparing the numerical results obtained with those given in the literature. For this purpose, the formulae derived were transformed from the cylinder to the disk case by eliminating the axial stresses. The equations derived in [10, 22] for stresses in rotating disks

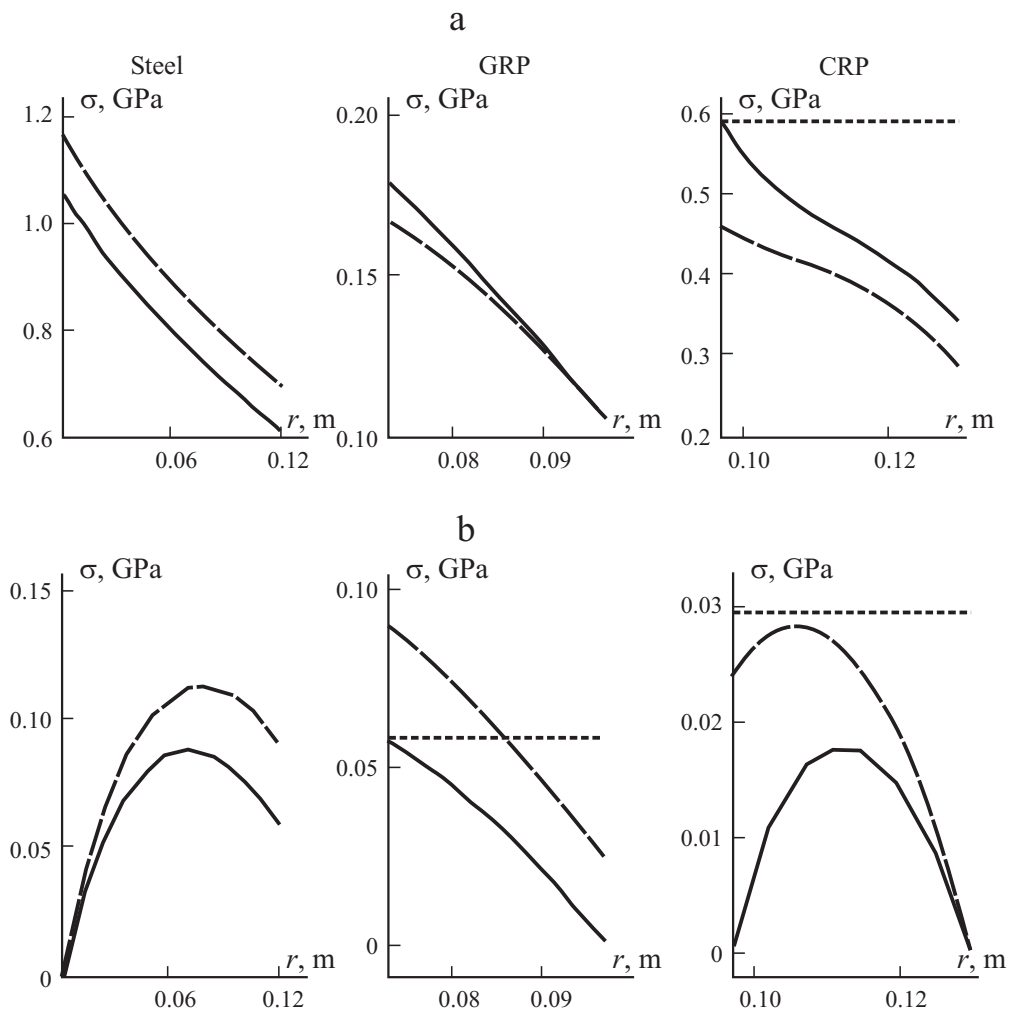

Fig. 1. Comparison of circumferential (a) and radial (b) stresses in disks and cylinders of hybrid steel–GRP–CRP flywheels. (——) — stresses in the cylinder, (— — —) — stresses in the disk; (- - -) — circumferential (a) and radial (b) tensile strengths.

without temperature changes were employed together with formulae for pure thermal stresses in the disks investigated in [23]. All results from the equations mentioned correspond to the equations transformed for disks. The integral characteristics of stress state in the cylinder calculated by using the relations obtained coincided with the value of the kinetic energy accumulated in the rotating cylinder (such an estimation of accuracy of the calculated stress state was suggested in [24]).

4.2 Comparison of stresses calculated using the hypotheses of plane stress (disks) and plane strain (cylinders) states. As is well known, the stresses and displacements in disks can be expressed by rather simple analytical expressions. Therefore, it is of interest to clarify if it is advisable to use the more complicated relations for stress calculations in cylinders, i.e., we must estimate the difference between the stresses in disks and cylinders (radial and circumferential) with the same radial dimensions and calculate the axial stresses in cylinders.

As was shown by numerous calculations, the difference between plane stress (disk approach) and plain strain states in a rotating single (uniform) cylinder is negligible (disregarding the appearance of axial stresses, which are relatively low — about 0.3-0.4 of the maximum radial stresses in thick cylinders).

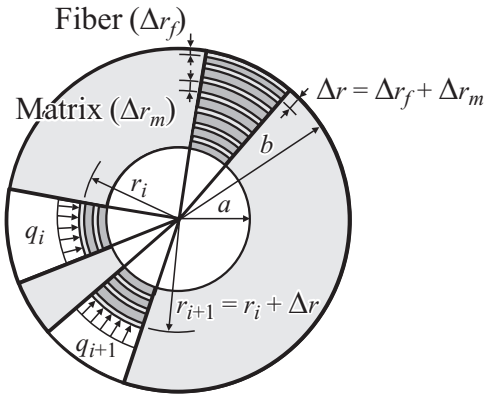

Fig. 2. Circular model of a wound cylinder.

But the situation is changed in the case of compound cylinders. Whereas the difference between the stresses due to rotation in the disc and cylinder is not great, the thermal stresses can differ considerably. The sum of the stresses presented in Fig. 1 shows that the disk approach gives smaller circumferential stresses and higher radial ones. As the radial strength in most cases is the decisive factor for finding dimensions, the use of only disk equations can lead to a design of thinner cylinders. Accordingly, such cylinders will store less energy. In our example, the radial disk stresses are around 50 percent higher in the GRP cylinder and more than 60 percent higher in the CRP cylinder than those calculated with the plane-strain assumption.

The axial stresses in cylinders, in principle, can be the reason for axial failure. But in our case, they are not critical[1]. Thus, the transition from a disk to a cylinder design is vital for steel-GRP-CRP flywheels. The use of disk equations for them can lead to essentially incorrect results.

5. Initial Stresses in a Wound Cylinder due to the Force Winding

5.1. Description of the model. The efficiency of the use of press fit in joining several composite rings in one thick rim to avoid the preliminary delamination during rotation of disk-type flywheels due to the radial tensile stresses is well known [13, 15, 16]. This procedure requires a separate manufacture of rings and their careful preparation, and it becomes complicated with increasing axial length of the rim. The main aim of the present investigation is to estimate the efficiency of winding with high tensioning (force winding) for increasing the stored kinetic of a hybrid flywheel — cylinder. Thus, the dangerous radial stresses generated in the flywheel during rotation is suppressed not by means of sequential press fits of previously manufactured rings, but by generating compressive radial stresses directly during the winding stage of the flywheel.

The model for stress calculations in the wound part was evidently first considered in [26].This model, as applied to composite winding, was considered in [27, 28]. According to it, the winding operation is represented as successive mounting of thin circular layers onto a mandrel and then onto the previous layer under a tension equal to the winding tensioning of the tape. This is illustrated in Fig. 2. The linearly elastic circular winding model gives a possibility of accounting the most important factor, namely the anisotropy of deformational properties of the semi-fabricated material. The model describes the traditional

[1] The calculations were performed for a hybrid flywheel consisting of a steel cylinder ($a_1 = 0.048$ m, $c_1 = 0.65$, and density = 7850 kg · m^{-3}), a GRP cylinder ($c_2 = 0.754$; properties of the S2 - glass/epoxy XP251S[25]: density = 1980 kg · m^{-3}, $E_\theta = 51$ GPa, $E_r = 17$ GPa, $E_z = E_r$, $\nu_{r\theta} = 0.25$, $\nu_{rz} = 0.32$, the radial strength in tension $F_r^+ = 58$ MPa, and the hoop strength in tension $F_\theta^+ = 1779$ MPa), and a CRP cylinder ($c_3 = 0.746$; properties of the GY70 - carbon/epoxy 934 [35]: density = 1590 kg · m^{-3}, $E_\theta = 294$ GPa, $E_r = 6.4$ GPa, $E_z = E_r$, $\nu_{r\theta} = 0.23$, $\nu_{rz} = 0.30$, the radial strength in tension $F_r^+ = 29$ MPa, and the hoop strength in tension $F_\theta^+ = 589$ MPa).

winding process qualitatively and, in the case of winding with *in situ* curing, also quantitatively if the properties of the cured material are known.

At the moment when the outer radius of the successive wound circuit lies on the running radius r, the stresses at the outer radius are equal to

$$\sigma_r = 0, \quad \sigma_\theta = \sigma_\theta^0, \tag{14}$$

where σ_θ^0 is the stress applied to the band during winding, which is generated by a tensioning device. The stresses vary with the pressure q_i created during the winding of each successive turn:

$$\Delta\sigma_r(r_i) = -q_i = -\frac{\Delta r_{i+1}}{r_i}\sigma_\theta^0(r_{i+1}) \quad \text{at} \quad r_i = r_{i+1} - \Delta r_{i+1}, \tag{15}$$

where r_{i+1} is the current outer radius, Δr is the layer thickness, and q_i is the external pressure at an ith turn.

The stresses in a cylinder wound from $r = r$ to $r = r_i$ may be represented as the sum of increments obtained at the given radius r due to winding with the successive interference fit of the thin rings. During the interference fit, each ring creates a radial pressure q, as seen in Eq. (15). Thus, the stresses in the wound cylinder can be represented as follows:

$$\begin{aligned}\sigma_r(r, r_i) &= \Delta\sigma_r(r, r+\Delta r) + \Delta\sigma_r(r, r+2\Delta r) + \ldots + \Delta\sigma_r(r, r_i),\\ \sigma_\theta(r, r_i) &= \sigma_\theta^0(r) + \Delta\sigma_\theta(r, r+\Delta r) + \Delta\sigma_\theta(r, r+2\Delta r) + \ldots + \Delta\sigma_\theta(r, r_i).\end{aligned} \tag{16}$$

In determining the stresses at the increments $\Delta\sigma_r$ and $\Delta\sigma_\theta$, the ring already wound can be considered as a quasi-uniform, cylindrically orthotropic, linearly elastic body loaded with an external pressure q, with boundary conditions at the interface between the mandrel and the wound body reflecting the continuity of radial stresses and displacements.

5.2 Winding stresses. Let us introduce the dimensionless radii

$$\zeta_w = r/a_2, \quad m_i = r_i/a_2, \tag{17}$$

where a_2 is the inner radius of the wound ring, equal to the outer radius b_1 of the mandrel, r is the current radius of the wound ring, and r_i is the outer radius of the wound ring during winding. Using the results obtained in [22] for the plane stress state of a pressure-loaded compound two-layer ring, the expressions for stress increments in a wound linearly elastic body (see Eq. (16)) can be presented the form

$$\begin{aligned}\Delta\sigma_r(\zeta_w, m_i) &= -q(\eta_w\zeta_w^{\kappa_w - 1} + \zeta_w^{-\kappa_w - 1})\frac{1}{m_i^{-\kappa_w - 1} + \eta_w m_i^{\kappa_w - 1}},\\ \Delta\sigma_\theta(\zeta_w, m_i) &= -q\kappa_w(\eta_w\zeta_w^{\kappa_w - 1} + \zeta_w^{-\kappa_w - 1})\frac{1}{m_i^{-\kappa_w - 1} + \eta_w m_i^{\kappa_w - 1}},\end{aligned} \tag{18}$$

$$\eta_w = \left(\kappa_w + \frac{\gamma_1}{C_{11}^{(w)}} - \frac{C_{21}^{(w)}}{C_{11}^{(w)}}\right) \Bigg/ \left(\kappa_w - \frac{\gamma_1}{C_{11}^{(w)}} + \frac{C_{21}^{(w)}}{C_{11}^{(w)}}\right), \tag{19}$$

$$\kappa_w = \sqrt{C_{22}^{(w)}/C_{11}^{(w)}}, \tag{20}$$

where $C_{ij}^{(w)}$ are the elements of compliance matrix (3), and γ_1 is the compliance of the mandrel loaded with external pressure. The parameter γ_1 for a mandrel made of an isotropic material takes the form

$$\gamma_1 = \frac{u_1(b_1)}{b_1\sigma_r(b_1)} = \frac{\bar{u}_1(b_1)}{\sigma_r(b_1)} = \frac{1}{E^{(1)}}\left(\frac{m_1^2+1}{m_1^2-1} - \nu^{(1)}\right), \tag{21}$$

where $E^{(1)}$ and $\nu^{(1)}$ are the elastic modulus and Poisson ratio of the mandrel material, and $m_1 = b_1/a_1$ is the ratio of external to internal radii of the mandrel.

If the mandrel is compound, e. g., consists of two cylinders, first the parameter η_2 [analogous to η_w (19)] is calculated:

$$\eta_2 = \left(\kappa_2 + \frac{\gamma_1}{C_{11}^{(2)}} - \frac{C_{21}^{(2)}}{C_{11}^{(2)}}\right) \Bigg/ \left(\kappa_2 - \frac{\gamma_1}{C_{11}^{(w)}} + \frac{C_{21}^{(2)}}{C_{11}^{(2)}}\right), \quad \kappa_2 = \sqrt{C_{22}^{(2)}/C_{11}^{(2)}}. \tag{22}$$

In particular, $C_{ij}^{(2)} = C_{ij}^{(w)}$, if, after winding the second cylinder, a third cylinder is wound using another material and we calculate stresses in that, third cylinder.

From the known parameter η_2, we can calculate the radial compliance γ_2 of the compound two-layer cylinder:

$$\gamma_2 = C_{11}^{(2)}\left(k_2\frac{\eta_2 m_2^{2k_2}+1}{\eta_2 m_2^{2k_2}-1} + \frac{C_{21}^{(2)}}{C_{11}^{(2)}}\right). \tag{23}$$

Then the parameter η_w can be calculated and used for determining stress increments in the next (third) cylinder. This procedure can be extended to any number of cylinders.

Taking into account the very small thickness q of the wound tape, Eq. (15) can be presented in the form

$$q(m_i) = \frac{\sigma_\theta(m_i)dm_i}{m_i}. \tag{24}$$

Substituting (24) into (18) and replacing the summation in (16) with integration, the expressions for circumferential and radial stress distributions in the wound cylinder with the radius ratio m_2 can be written in the form

$$\sigma_r(\zeta_w, m_2) = -(\eta_w\zeta_w^{\kappa_w-1} + \zeta_w^{-\kappa_w-1})\int_{\zeta_w}^{m_2}\frac{\sigma_{\theta i}^0(m_i)dm_i}{m_i^{-\kappa_w}+\eta m_i^{\kappa_w}},$$
$$\sigma_\theta(\zeta_w, m) = \sigma_\theta^0(\zeta_w) - \kappa_w(\eta_w\zeta_w^{\kappa_w-1} + \zeta_w^{-\kappa_w-1})\int_{\zeta_w}^{m_2}\frac{\sigma_{\theta i}^0(m_i)dm_i}{m_i^{-\kappa_w}+\eta m_i^{\kappa_w}}, \quad 1 \le \zeta_w \le m_2. \tag{25}$$

5.3. Discussion of the winding model. The use of relations (25) in the present investigation is connected with the following assumptions:

(a) the winding material is linearly elastic in the hoop and radial directions;

(b) only the hoop and radial stresses are considered, neglecting the axial stresses;

(c) the layers wound do not lose their circular alignment during winding;

(d) the part of stress state generated by winding with tensioning does not change at a later time.

Let us consider all of them. The assumption of linear elasticity in the hoop direction looks reasonable if there are not buckling or waviness of layers during winding. The only work , known to the authors, which is devoted to experimental investigations of the radial compliance of composite wound parts during its manufacture is [29]. In this work, the radial compliance at the initial stages of the technological process was measured on specimens made from a band of glass fabric impregnated with epoxy resin, which was wound with a 200 N/cm tensioning. The end of the band was attached with an epoxy compound, and then strain gages were glued. The specimen was placed into a cylinder, which was then filled with glycerine heated to 130°C.

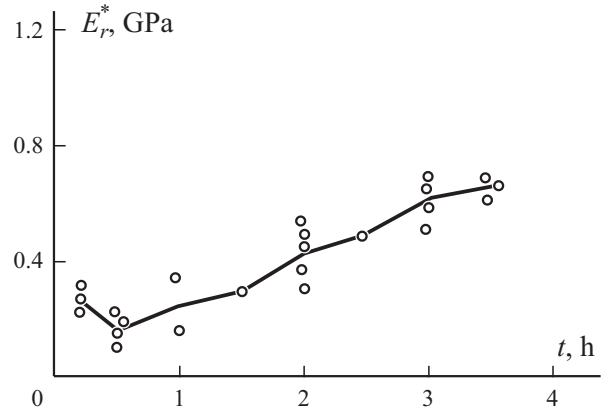

Fig. 3. Radial plain-strain modulus E_r^* of a glass fabric prepreg impregnated with epoxy at 120°C as a function of time t [29].

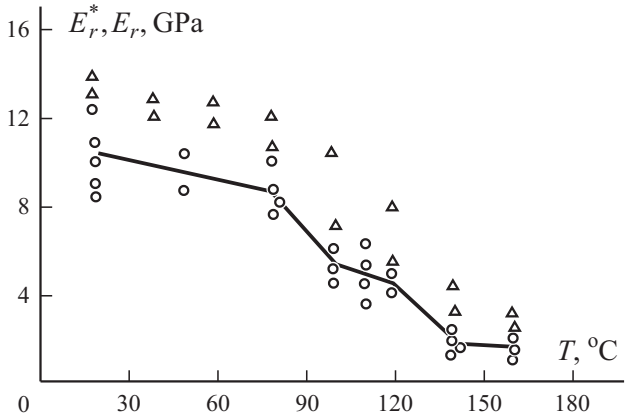

Fig. 4. Radial and plain-strain moduli, E_r^* and E_r, of a cured glass fabric/epoxy prepreg as functions of temperature T [29], determined on cylindrical (○) and flat (△) specimens.

After assembling, the cylinder was placed into a thermostat filled with glycerine, and the experiment was carried out at 120°C. The pressure increment was 0.5 MPa, and the maximum load was 25 MPa. Even at early stages of manufacture of GRP, when the resin was softened, a practically linear dependence between the load and strain was observed, which is explained by the volumetric stress state of the cylinder.

This allows us to consider the cylinder material as linearly elastic even at early stages of its manufacture, with the transversal modulus of plane strain E_r^*. The experimentally determined variations in E_r^* with time at this stage are shown in Fig. 3, where the solid line corresponds to the mean value of the modulus. At the beginning, a decrease in E_r^* is seen, which is caused by softening of the resin as a result of heating. Then E_r^* increases during the polymerization. The minimum value of $E_r^* = 0.14$ GPa corresponds to the initial heating to 120°C.

For examining the temperature dependence of the modulus E_r^* in completely cured articles, the same investigation was carried out on cured cylinders. The specimens were cured in thermostats at 120°C during 20 hours. A uniform distribution

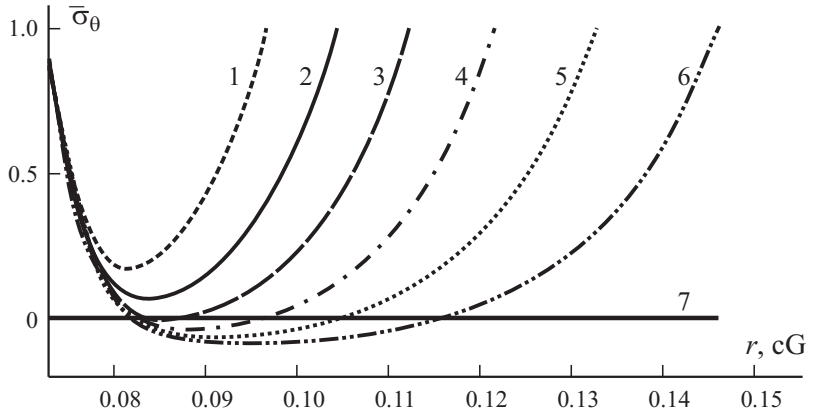

Fig. 5. Relative winding hoop stresses $\overline{\sigma}_\theta$ in GRP cylinders with relative dimensions $cG =$ 0.754 (1), 0.7 (2), 0.65 (3), 0.6 (4), 0.55 (5), 0.5 (6), and 0 (7).

of temperature was ensured by holding them at a given temperature for 30 min. The temperature dependence of the radial plain-strain modulus E_r^* is presented in Fig. 4. In this figure, the results of determining the elastic modulus E_r on prismatic specimens are also presented (with triangles). The latter were cut from 100-mm-thick rings. The strains were measured using gages with a 20-mm base. The data presented in [29] not only confirm the possibility of using the linearly elastic model in considering cylinder winding, but they also give an indication of the order of magnitude of the radial (transverse) modulus of glass fibers impregnated with resin during different stages of composite curing. It is likely that for rovings this modulus can be higher.

The axial stresses for a cylinder with clamped ends can be obtained from the condition $\varepsilon_z = 0$ as

$$\sigma_z = -\frac{1}{C_{33}^{(w)}}\left(C_{23}^{(w)}\sigma_r + C_{13}^{(w)}\sigma_\theta\right), \tag{26}$$

where σ_r and σ_θ are expressed from Eq. (25).

The calculation of these stresses seems questionable because of the absence of even approximate values for $\nu_{rz}^{(w)}$ and $\nu_{\theta z}^{(w)}$. Taking into account their small magnitude and the approximate character of calculations, the axial stresses arising during winding were neglected.

For estimating the assumption (c), let us consider the distribution of hoop stresses appearing during winding by using Eqs. (25). On winding with a constant tensioning, the hoop stresses in a wound cylinder are proportional to the tension $\sigma_\theta^0(m_i) = \text{const}$. The relative values of these stresses in a GRP cylinder wound on a cylindrical steel mandrel are shown in Fig. 5. The dimensions of the steel mandrel and the deformational properties of the GRP are indicated in the remark to Fig. 1 (except for the radial modulus, which corresponds to its possible value for an uncured composite, 0.4 GPa). As can be seen from these data, in a thick cylinder, the stresses in the inner part of the cylinder can be compressive. Practically this means a loss in the initial tensioning and the buckling of fibers if the composite at the winding stage has a low radial modulus. It is interesting that, with increasing cylinder thickness, the maximum compressive stresses increase insignificantly and reach about $-0.1\sigma_\theta^0$, but the growth of the compressed region is significant. With decreasing radial modulus, the minimum thickness of the cylinders, corresponding to the appearance of compressed layers, also decreases (the relative dimensions of the cylinders increase). The minimum values of the radial modulus of GRP ensuring the minimum value of tensioning in wound cylinders equal to zero are presented in Fig. 6 (the dimensions of the steel cylinder-mandrel and the hoop modulus of GRP correspond to those utilized for

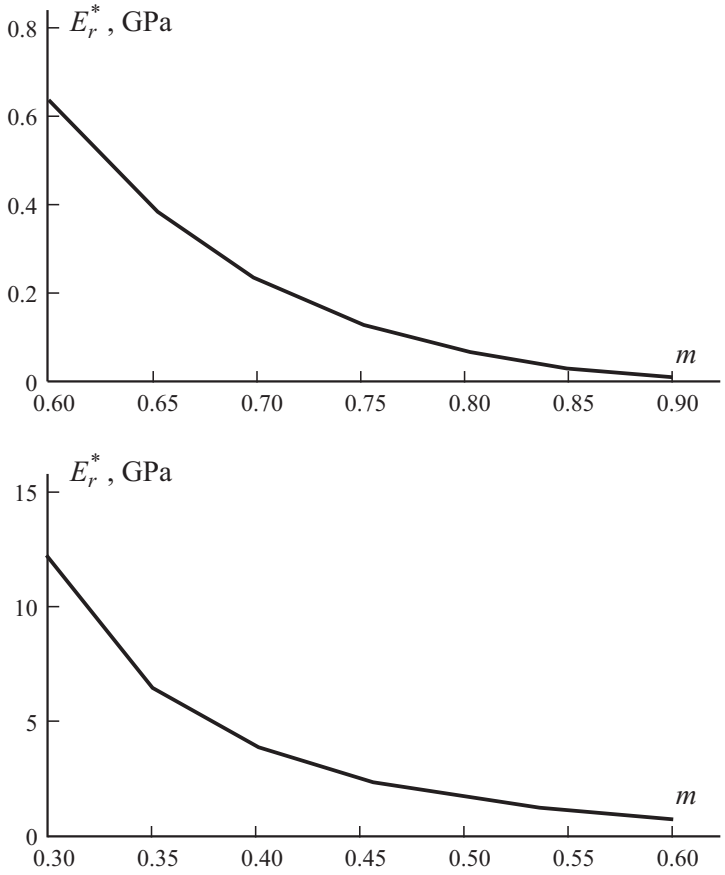

Fig. 6. Radial modulus E_r^* of GRP corresponding to the appearance of zero tension in cylinders wound with a constant tensioning; m is the relative dimension.

Fig. 5). Thus, to avoid the buckling of fibers and their waviness in thick wound cylinders, the composite at the winding stage must be sufficiently rigid in the radial direction. As can be seen from Fig. 5, to avoid compression stresses in thick wound cylinders of GRP ($cG = 0.3$), the radial modulus of the winding material must be close to the radial modulus of the fully cured material (17GPA). It is obvious that this requirement for the radial modulus is superfluous. At a certain value of radial modulus, the winding composite is able to react to a compressive load that is sufficiently low (see Fig. 4). Therefore, it is desirable to find the means for increasing the radial modulus of the winding material. The *most* efficient method for solving this problem is the use of winding with continuous *in situ* curing.

5.4 Filament winding with *in situ* curing. The traditional wet filament winding and the curing of thick thermoset composites can lead to many quality problems, such as wavy fibers due to the loss of fiber tensioning, a heat damage due to uncontrolled exotermic reactions, an excessive porosity due to improper consolidation, and unacceptably high residual thermal stresses, which reduce the in-service load-carrying capability. All these problems, except the heat damage, are in some way related to the internal distribution of stresses during winding, consolidation, and cure.

The new method follows the basic ideas of continuous consolidation and cure of thermosetting resins during winding described previously in [30-33]. It involves wet winding and heating of the material when it is applied to a mandrel. The heat supply to the material can be provided by internally heating the mandrel, with internal infrared heat lamps, and with space heaters. But often not all these methods are necessary for a proper temperature control. The internal mandrel heaters do most of the heating and are probably the only heat source needed [32].

In [34] it was shown that, after the initial start-up period of winding has passed and the thickness of material has built up to some appreciable level, the curing material is insulated to a large degree from the heated mold surface. Thus, the energy for propagating the thermal and cure fronts is obtained directly from the exothermic cure reaction. The curing will continue as long as a fresh material is added to the outer surface; the process becomes self-sustained. The final cure of epoxy resins is achieved in a long time, but a significant degree of cure (about 0.8) may be achieved in an acceptable time, especially at high temperatures (50 min at 145°C) [35]. The standard rule of thumb is that the gel time is halved at about every 10°C increase in temperature [32].

By winding with continuous curing, the gelled thickness increases in such a way that it remains about 5 mm below the winding surface [31]. The inner layer fibers are held in place, the excessive resin flow is prevented from being squeezed out, and the loss in fiber tensioning is therefore minimized. As were shown experimentally in [32], this method yielded a high fiber volume fraction, no fiber waviness, a low content of voids, low residual stresses, and a uniform consistency throughout the material in wound rings with relative dimensions up to 0.49. In [34], a good-quality ring with relative dimension 0.33 was manufactured with even compressive residual radial stresses.

Thus, the application of winding with *in situ* curing gives a possibility of employing the assumptions (a), (c), and (d) of the winding model (see above).This justifies the use of relations (25) for estimating the possible increase in the energy storage capacity of hybrid steel-composite cylindrical flywheels on applying high tensioning during their winding with *in situ* curing. It is significant that the degree of cure in a cylinder during filament winding is higher than in a ring at equal heating, because of the prolonged intrinsic thermal treatment time.

6. Summary and Conclusions

In the first part of the study, the basic relations for estimating the efficiency of force winding of hybrid steel-composite cylindrical flywheels were considered and discussed. It was shown that the passage from a plane stress to a plain strain state is necessary in calculating the hoop and radial stresses in compound cylinders. The application of a linearly elastic model for calculating the winding stresses may be attractive when winding with continuous *in situ* curing is used.

REFERENCES

1. Proceedings. Flywheel Technology Symposium, November 10-12, 1975, Lawrence Livermore Laboratory, Berkeley, California (1975).
2. Proceedings. Flywheel Technology Symposium, October 5-7, 1977, U.S. Department of Energy, San Francisco, California (1977).
3. Proceedings. Flywheel Technology Symposium, October 1980, U.S. Department of Energy, ASME, LLNL, Scottsdale, Arizona (1980).
4. Proceedings. Flywheel Energy Storage Workshop, October 1995, CONF- 9510242, U.S. Department of Energy (1995).
5. S. Ashley, Mech. Eng., **115,** No. 10, 44-51 (1993).
6. B. Koch, Electr. World, 44-47 (December 1997).
7. A Summary of the State of the Art of Superconducting Magnetic Energy Storage Systems, Flywheel Energy Storage Systems and Compressed Air Energy Storage Systems. Sandia Report, SAND99-1854 (July 1999).
8. J. G. Bitterly, "Technology. past, present and 21st century projections," IEE AES Systems Mag., 13-16 (August 1998).
9. C. E. Bakis, "Batteries for the 21st century: composite flywheels," Eng. Mater. Systems, **1,** No. 1 (1998).
10. G. Genta, Kinetic Energy Storage, Butterworths & Co. Ltd. (1985).
11. K. Shintarou, "Flywheel," in: Comprehensive Composite Material. Vol. 6, Ch. 6.29, Elsevier Sci. Ltd., (2000), pp. 571-580.
12. E. D. Reedy Jr., "A composite-rim flywheel design," SAMPE Quart., 1-6 (April 1978).

13. S. M. Arnold, A. F. Saaleb, and N. R. Al-Zoubi, Deformation and Life Analysis Of Composite Flywheel Disk And Multi-Disk Systems, NASA/TM – 2001-210578 (January 2001).
14. S. K. Ha and D.-J. Kim, "Optimal design of a hybrid composite flywheel rotor using finite element methods," in: Proceedings of the 44th SAMPE Symposium, May 23-27, 1999, SAMPE, Covina, CA (1999), pp. 2119-2131.
15. D. M. Ries and J. A.Kirk, "Design and manufacturing for a composite multi-ring flywheel," in: Proceedings of the 27th Intersociety Energy Conversion Engineering Conference, August 3-7, 1992. Vol. 4, San Diego, CA (1992), pp. 43-47.
16. R. A. Huntington, J. A. Kirk, Stress Redistribution for Multi-Ring Flywheel, ASME Publication 77-WA/DE-26, (1977).
17. R. F. Post and S. F. Post, "Flywheels," Scient. American, **229,** No. 6, 17-23 (December 1973).
18. W. M. Brobeck, "Flywheel development for the electric power research institute," in: Proceedings. Flywheel Technology Symposium, CONF-771053, October 1977, U.S. Department of Energy (1977), pp. 183-192.
19. C. W. Gabrys, C. E. Bakis, "Design and testing of composite flywheel rotors," in: S. J. Hooper, (ed.), Composite Materials: Testing and Design. Vol. 13, ASTM STP 1242, ASTM (1997), pp. 1-22.
20. S. K. Ha and D.-J. Kim, Optimum Design of Multi-Rim Composite Flywheel Rotor Using a Modified Generalized Plane Strain Assumption, KEPRI Technical Report TR.96TJ48.E2000.199, 1999.5.
21. I. Cruz, F. Arias, R. P. Giffe, L. Garsia Tabares, J. I. Iglesias, Marcos Lafoz, I. V. Marquez de Prado, and G. Portnov, "Design, construction, and test of a new 50-kW high-speed flywheel for wind/disel systems application," in: Proceedings. European Wind Energy Conference, 16-19 June, 2003, Madrid (2003), pp. 10.
22. S. G. Lehnitskii, Anisotropic Plates [in Russian], Moscow (1957).
23. V. V. Bolotin and K. S. Bolotina, "Thermoelastic problem of a circular cylinder of reinforced multilayer material," Polym. Mech., **3,** No. 1, 93-96 (1967).
24. G. G. Portnov, "Assesment of the energy storage capacity of rotating bodies by integral characteristics of their stress state," Probl. Prochn., No. 2, 7-12 (1987).
25. C. Kirchner Lapp, "Design alowable substantion," in: S. T. Peters (ed.), Handbook of Composites, Chapman & Hall, London (1998), pp. 758-777.
26. R. V. Southwell, An Introduction to the Theory of Elasticity for Engineers and Physicists, Oxford, 1936, pp.510
27. Y. M. Tarnopol'skii and G. G. Portnov, "Variation of prestress in filament-wound glass-reinforsed plastics," Polym. Mech., **2,** No. 2, 172-175 (1966).
28. C. Y. Liu and C. C. Chamis, "Residual stresses in filament wound laminates and optimum programmed winding tension," in: Proceedings of 20th Annual Technical Conference, Section 5-D, Reinforced Plastics Div., Soc. Plastics Ind., New York (1965), pp. 1-10.
29. V. L. Blagonadezin, V. P. Nikolaev, and V. G. Perevozhchikov, "Investigation of the transverse compliance of wound GRP products," in: V.V. Bolotin (ed.), Transactions of Moscow Institute for Energy. Dynamic and Strength of Machines, Iss. 101 [in Russian] (1972), pp. 36-40.
30. S. R. White and C. Kim, "A simultaneous lay-up and *in situ* cure process for thick composites," in: Proceedings of the American Society for Composites, 7th Technical Conference, Technomic, Lancaster, PA (1992), pp. 80-89.
31. V. N. Korotkov, Y. A. Chekanov, and B. A. Rozenberg, "The simultaneous process of filament winding and curing for polymer composites," Compos. Sci. Technol., **47,** 383-388 (1993).
32. C. W. Gabrys and C. E. Bakis, "Fabrication of thick filament wound carbon epoxy rings using *in situ* curing: manufacturing and quality," in: Proceedings of the American Society for Composites, 9th Technical Conference, September 20-22, 1994, Delaware (1994), pp.1090 – 1097.
33. C. Kim, H. Teng, I. Tucker, and S. R.White, "The continuous curing process for thermoset polymer composites. Pt. 1. Modelling and demonstration," J. Compos. Mater., **29**, 1222-1253 (1995).
34. C. Kim and S. R. White, "Continuous curing and induced thermal stresses of a thick filament wound composite cylinder," J. Reinf. Plast. Compos., **20**, No. 2 (2001).
35. D. J. O'Brien, P. T. Mather, and S. R. White, "Viscoelastic properties of an epoxy resin during cure," J. Compos. Mater., **35**, No. 10 (2001).